

Non-commutative time-frequency tomography

V.I. Man'ko*and R.Vilela Mendes

*Grupo de Física-Matemática, Complexo Interdisciplinar
Universidade de Lisboa
Av. Prof. Gama Pinto, 2, 1699 Lisboa Codex, Portugal*

Abstract

The characterization of non-stationary signals requires joint time and frequency information. However, time (t) and frequency (ω) being non-commuting variables, there cannot be a joint probability density in the (t, ω) plane and the time-frequency distributions, that have been proposed, have difficult interpretation problems arising from negative or complex values and spurious components. As an alternative we propose to obtain time-frequency information by looking at the marginal distributions along rotated directions in the (t, ω) plane. The rigorous probability interpretation of the marginal distributions avoids all interpretation ambiguities. Applications to signal analysis and signal detection are discussed as well as an extension of the method to other pairs of non-commuting variables.

1 Introduction

Non-stationary signals have a time-dependent spectral content, therefore, an adequate characterization of these signals requires joint time and frequency information. Among the many time-frequency (quasi)distributions[1] [2] that have been proposed, *Wigner-Ville's* (WV)[3] [4]

$$W(t, \omega) = \int f\left(t + \frac{u}{2}\right) f^*\left(t - \frac{u}{2}\right) e^{-i\omega u} du \quad (1)$$

*on leave from the P. N. Lebedev Physical Institute, Moscow, Russia

for an analytic signal $f(t)$, is considered to be optimal in the sense that it satisfies the marginals, it is time-frequency shift invariant and it possesses the least amount of spread in the time-frequency plane.

However, the WV distribution has, in general, positive and negative values and may be non-zero in regions of the time-frequency plane where either the signal or its Fourier transform vanish. Therefore, despite the fact that the WV distribution is an accurate mathematical characterization of the signal, in the sense that it can be inverted by

$$f(t)f^*(t') = \frac{1}{2\pi} \int W\left(\frac{t+t'}{2}, \omega\right) e^{i\omega(t-t')} d\omega \quad (2)$$

its interpretation for signal detection and recognition is no easy matter, because of the negative and "spurious" components. The origin of this problem lies in the fact that t and ω being non-commuting variables, they cannot be simultaneously specified with absolute accuracy and, as a result, there cannot be a joint probability density in the time-frequency plane. Therefore no joint distribution, even if positive[5], may be interpreted as a probability density.

Looking back at the original motivation leading to the construction of the time-frequency distributions, namely the characterization of non-stationary signals, we notice that we are asking for more than we really need. To characterize a non-stationary signal what we need is time and frequency-dependent information, not necessarily a joint probability density, a mathematical impossibility for non-commuting variables. The solution is very simple. The time density $|f(t)|^2$ projects the signal intensity on the time axis and the spectral density $|f(\omega)|^2$ projects on the frequency axis. To obtain the required time-frequency information, all we need is a family of time and frequency functions $s_\xi(t, \omega)$, depending on a parameter ξ , which interpolates between time and frequency. Projecting the signal intensity on this variable, that is, computing the density along the s_ξ -axis, one obtains a function

$$M(s, \xi) = |f(s_\xi)|^2 \quad (3)$$

that has, for each ξ , a probability interpretation. The simplest choice for s_ξ is a linear combination

$$s = \mu t + \nu \omega \quad (4)$$

the parameter ξ being the pair (μ, ν) . For definiteness we may choose

$$\begin{aligned} \mu &= \frac{\cos \theta}{T} \\ \nu &= \frac{\sin \theta}{\Omega} \end{aligned} \quad (5)$$

T, Ω being a reference time and a reference frequency adapted to the signal to be studied. The function $M(s, \theta)$ interpolates between $|f(t)|^2$ and $|f(\omega)|^2$ and, as we will prove below, contains a complete description of the signal. For each θ the function $M(s, \theta)$ is strictly positive and being a bona-fide probability (in s) causes no interpretation ambiguities. A similar approach has already been suggested for quantum optics[6] and quantum mechanics[7] [8] [9], the non-commuting variable pairs being respectively the quadrature phases (a_r, a_i) and the position-momentum (q, p) .

This approach, in which to reconstruct an object, be it a signal in signal processing or a wave function in quantum mechanics, one looks at its probability projections on a family of rotated axis, is similar to the *computerized axial tomography* (CAT) method. The basic difference is that in CAT scans one deals with a pair (x, y) of commuting position variables and here we deal with a plane defined by a pair of non-commuting variables. For this reason we call the present approach *non-commutative tomography* (NCT).

The paper is organized as follows. In Section 2 we construct the NCT signal transform and show its positivity and normalization properties. We also establish the invertibility of the transformation, which shows that it contains a complete description of the signal and establish its relation to the WV distribution. Because the NCT transform involves the square of the absolute value of a linear functional of the signal, it is actually easier to compute than bilinear transforms like WV.

In Section 3 we work out the analytical form of the NCT transform for some signals and also display the $M(s, \theta)$ in some examples. We also deal with the problem of using NCT to detect the presence of signals in noise for small *signal to noise ratios* (SNR). Here the essential observation is that, for small SNR, the signal may be difficult to detect along t or ω , however, it is probable that there are other directions on the (t, ω) plane along which detection might be easier. It is the consistent occurrence of many such directions that supplies the detection signature.

Finally in Section 4 we point out that the NCT approach may also be used for other pairs of non-commuting variables of importance in signal processing. As an example we work out the relevant formulas for the scale-frequency pair.

2 Non-commutative time-frequency tomography

Because the Fourier transform of a characteristic function is a probability density, we compute the marginal distribution for the variable $s = \mu t + \nu \omega$ using the characteristic function method. Frequency and time are operators acting in the Hilbert space of analytic signals and, in the time-representation, the frequency operator is $\omega = -i\partial/\partial t$. The characteristic function $C(k)$ is

$$C(k) = \langle e^{ik(\mu t + \nu \omega)} \rangle = \int f^*(t) e^{ik(\mu t - i\nu \partial/\partial t)} f(t) dt \quad (6)$$

where $f(t)$ is a normalized signal

$$\int |f(t)|^2 dt = 1$$

The Fourier transform of the characteristic function is a probability density

$$M(s, \mu, \nu) = \frac{1}{2\pi} \int C(k) e^{-iks} dk \quad (7)$$

After some algebra, one obtains the marginal distribution (7) in terms of the analytical signal

$$M(s, \mu, \nu) = \frac{1}{2\pi|\nu|} \left| \int \exp \left[\frac{i\mu t^2}{2\nu} - \frac{its}{\nu} \right] f(t) dt \right|^2 \quad (8)$$

with normalization

$$\int M(s, \mu, \nu) ds = 1 \quad (9)$$

For the case $\mu = 1, \nu = 0$, it gives the distribution of the analytic signal in the time domain

$$M(t, 1, 0) = |f(t)|^2 \quad (10)$$

and for the case $\mu = 0, \nu = 1$, the distribution of the analytic signal in the frequency domain

$$M(\omega, 0, 1) = |f(\omega)|^2 \quad (11)$$

The family of marginal distributions $M(s, \mu, \nu)$ contains complete information on the analytical signal. This may be shown directly. However it

is more interesting to point out that there is an invertible transformation connecting $M(s, \mu, \nu)$ to the Wigner-Ville quasidistribution, namely

$$M(s, \mu, \nu) = \int \exp[-ik(s - \mu t - \nu\omega)] W(t, \omega) \frac{dk d\omega dt}{(2\pi)^2} \quad (12)$$

and

$$W(t, \omega) = \frac{1}{2\pi} \int M(s, \mu, \nu) \exp[-i(\mu t + \nu\omega - s)] d\mu d\nu ds \quad (13)$$

Therefore, because the WV quasidistribution has complete information, in the sense of Eq.(2), so has $M(s, \mu, \nu)$.

3 Examples

We compute the NCT transform $M(s, \mu, \nu)$ for some analytic signals:

(i) *A complex Gaussian signal*

$$f(t) = \left(\frac{\alpha}{\pi}\right)^{1/4} \exp\left[-\frac{\alpha}{2}t^2 + i\frac{\beta}{2}t^2 + i\omega_0 t\right] \quad (14)$$

It has the properties

$$\langle t \rangle = 0, \quad \langle \omega \rangle = \omega_0 \quad (15)$$

$$\begin{aligned} \sigma_t^2 &= \langle t^2 \rangle - \langle t \rangle^2 = \frac{1}{2\alpha} \\ \sigma_\omega^2 &= \langle \omega^2 \rangle - \langle \omega \rangle^2 = \frac{\alpha^2 + \beta^2}{2\alpha} \\ r &= \frac{2^{-1} \langle t\omega + \omega t \rangle - \langle t \rangle \langle \omega \rangle}{\sigma_\omega \sigma_t} = \frac{\beta}{\sqrt{\alpha^2 + \beta^2}} \end{aligned} \quad (16)$$

This signal minimizes the Robertson–Schrödinger uncertainty relation

$$\sigma_\omega^2 \sigma_t^2 \geq \frac{1}{4} \frac{1}{1 - r^2} \quad (17)$$

In quantum mechanics, it corresponds to a correlated coherent state [10] [11].

The NCT transform is

$$M(s, \mu, \nu) = \frac{1}{\sqrt{2\pi\sigma_s^2}} \exp\left[-\frac{(s - \bar{s})^2}{2\sigma_s^2}\right] \quad (18)$$

with parameters

$$\begin{aligned}\sigma_s^2 &= \frac{1}{2\alpha} |\nu(\alpha - i\beta) - i\mu|^2 \\ \bar{s} &= \omega_0 \nu\end{aligned}\quad (19)$$

For the case of $\mu = \frac{\cos \theta}{T}$, $\nu = \frac{\sin \theta}{\Omega}$, Eq.(19) shows how the initial Gaussian evolves along the θ axis, changing its maximum and width

$$\begin{aligned}\sigma_s^2 &= \frac{1}{2\alpha} \left| \frac{\sin \theta}{\Omega} (\alpha - i\beta) - i \frac{\cos \theta}{T} \right|^2 \\ \bar{s} &= \omega_0 \frac{\sin \theta}{\Omega}\end{aligned}\quad (20)$$

Thus, we have squeezing in the quadrature components and their correlation. In the case $\beta = 0$, one has a purely squeezed state[12] [13], which minimizes the Heisenberg uncertainty relation

$$\sigma_\omega^2 \sigma_t^2 \geq \frac{1}{4}\quad (21)$$

(ii) *A normalized superposition of two Gaussian signals*

$$f(t) = N_s \{A_1 f_1(t) + A_2 f_2(t)\}\quad (22)$$

where $f_i(t)$ is

$$f_i(t) = N_i \exp[-a_i t^2 + b_i t], \quad i = 1, 2\quad (23)$$

and

$$N_i = \left[\frac{a_i + a_i^*}{\pi} \right]^{1/4} \exp \left[-\frac{1}{8} \frac{(b_i + b_i^*)^2}{a_i + a_i^*} \right]\quad (24)$$

The superposition coefficients being complex numbers, the normalization constant N_s reads

$$N_s = \left(|A_1|^2 + |A_2|^2 + 2 \operatorname{Re} \left[A_1 A_2^* \int f_1(t) f_2^*(t) dt \right] \right)^{-1/2}\quad (25)$$

Computing the marginal distribution $M(s, \mu, \nu)$ by Eq.(8) we arrive at a combination of three Gaussian terms

$$\begin{aligned}M(s, \mu, \nu) &= N_s^2 \{ |A_1|^2 M_1(s, \mu, \nu) + |A_2|^2 M_2(s, \mu, \nu) \\ &\quad + 2 \operatorname{Re} [A_1 A_2^* M_{12}(s, \mu, \nu)] \}\end{aligned}\quad (26)$$

where we have the contribution of two real Gaussian terms

$$M_i(s, \mu, \nu) = \frac{1}{\sqrt{2\pi\sigma_i^2}} \exp\left[-\frac{(s - \bar{s}_i)^2}{2\sigma_i^2}\right], \quad i = 1, 2, \quad (27)$$

and the superposition of two complex Gaussians

$$M_{12}(s, \mu, \nu) = \frac{n_{12}}{\sqrt{2\pi\sigma_{12}^2}} \exp\left[-\frac{(s - \bar{s}_{12})^2}{2\sigma_{12}^2}\right] \quad (28)$$

The parameters of the real Gaussians are the dispersion

$$\sigma_i^2 = 2 \frac{|\nu a_i - \frac{i\mu}{2}|^2}{a_i + a_i^*} \quad (29)$$

and mean

$$\bar{s}_i = \nu \frac{\text{Im}(b_i a_i^*) + \text{Re}\left(\frac{\mu}{2\nu} b_i\right)}{\text{Re } a_i} \quad (30)$$

The parameters of the complex Gaussian are

$$\sigma_{12}^2 = 2\nu^2 \frac{\left(a_1 - \frac{i\mu}{2\nu}\right) \left(a_2^* + \frac{i\mu}{2\nu}\right)}{a_1 + a_2^*} \quad (31)$$

and

$$\bar{s}_{12} = \frac{i\nu}{a_1 + a_2^*} \left[b_2^* \left(a_1 - \frac{i\mu}{2\nu}\right) - b_1 \left(a_2^* + \frac{i\mu}{2\nu}\right) \right] \quad (32)$$

and the complex amplitude n_{12} of the complex Gaussian contribution is

$$n_{12} = \frac{\sigma_{12}}{\sqrt{2\pi}|\nu|} \exp\left[\frac{1}{4} \left(\frac{b_1^2}{a_1 - \frac{i\mu}{2\nu}} + \frac{b_2^{*2}}{a_2^* + \frac{i\mu}{2\nu}} \right) + \frac{\bar{s}_{12}^2}{2\sigma_{12}^2}\right] \quad (33)$$

(iii) *Finite-time signals*

Here we consider signals

$$f_i(t) = N_i e^{-a_i t^2 + b_i t}, \quad t_{2i} \leq t \leq t_{1i} \quad (34)$$

which vanish for all other times and compute the NCT for one signal and for the superposition of two such signals. The parameters a_i and b_i are complex numbers. The normalization constant is

$$\mathcal{N}_i = \sqrt{a_i + a_i^*} \exp \left[-\frac{(b_i + b_i^*)^2}{4(a_i + a_i^*)} \right] \left| \frac{\sqrt{\pi}}{2} \left[\operatorname{erfc} \left(\sqrt{a_i + a_i^*} \left[t_{2i} - \frac{b_i + b_i^*}{2(a_i + a_i^*)} \right] \right) - \operatorname{erfc} \left(\sqrt{a_i + a_i^*} \left[t_{1i} - \frac{b_i + b_i^*}{2(a_i + a_i^*)} \right] \right) \right] \right|^{-1/2} \quad (35)$$

where erfc is the function

$$\operatorname{erfc}(y) = \frac{2}{\sqrt{\pi}} \int_y^\infty e^{-x^2} dx \quad (36)$$

Using Eq.(8), we arrive at the following marginal distribution

$$M_i(s, \mu, \nu) = \frac{\mathcal{N}_i^2}{8|\nu|} \left| \operatorname{erfc} \left(\sqrt{a_i - \frac{i\mu}{2\nu}} \left[t_{2i} - \frac{\nu b_i - is}{2\nu a_i - i\mu} \right] \right) - \operatorname{erfc} \left(\sqrt{a_i - \frac{i\mu}{2\nu}} \left[t_{1i} - \frac{\nu b_i - is}{2\nu a_i - i\mu} \right] \right) \right|^2 \quad (37)$$

In the limit $t_{1i} \rightarrow -\infty$, $t_{2i} \rightarrow \infty$, the marginal distributions (37) reduce to the Gaussian distribution given by (27). In the case $a_i = 0$, $b_i = i\omega_i$, the distribution (37) describes a sinusoidal signal of finite duration. The normalization constant takes the limit value

$$N_i \implies (t_{2i} - t_{1i})^{-1/2} \quad (38)$$

For a superposition of two finite-time signals

$$f(t) = N_s \{A_1 f_1(t) + A_2 f_2(t)\}$$

with the signals $f_1(t)$ and $f_2(t)$ as in (34), the normalization constant is given by Eq.(25) with overlap integral

$$\int_{t_a}^{t_b} f_1(t) f_2^*(t) dt = \mathcal{N}_1 \mathcal{N}_2 \frac{\sqrt{\pi}}{2\sqrt{a_1 + a_2^*}} \exp \left[\frac{(b_1 + b_2^*)^2}{4(a_1 + a_2^*)} \right] \left\{ \operatorname{erfc} \left(\sqrt{a_1 + a_2^*} \left[t_a - \frac{b_1 + b_2^*}{2(a_1 + a_2^*)} \right] \right) - \operatorname{erfc} \left(\sqrt{a_1 + a_2^*} \left[t_b - \frac{b_1 + b_2^*}{2(a_1 + a_2^*)} \right] \right) \right\} \quad (39)$$

The marginal distribution for the superposition signal has the same form as Eq. (26) but with a changed normalization constant, the distributions $M_1(s, \mu, \nu)$ and $M_2(s, \mu, \nu)$ given by Eq. (37), and an interference term $M_{12}(s, \mu, \nu)$

$$\begin{aligned}
M_{12}(s, \mu, \nu) = & \frac{\mathcal{N}_1 \mathcal{N}_2}{8|\nu|} \left\{ \operatorname{erfc} \left(\sqrt{a_1 - \frac{i\mu}{2\nu}} \left[t_{21} - \frac{\nu b_1 - is}{2\nu a_1 - i\mu} \right] \right) \right. \\
& - \operatorname{erfc} \left(\sqrt{a_1 - \frac{i\mu}{2\nu}} \left[t_{11} - \frac{\nu b_1 - is}{2\nu a_1 - i\mu} \right] \right) \left. \right\} \\
& \times \left\{ \operatorname{erfc} \left(\sqrt{a_2 - \frac{i\mu}{2\nu}} \left[t_{22} - \frac{\nu b_2 - is}{2\nu a_2 - i\mu} \right] \right) \right. \\
& - \operatorname{erfc} \left(\sqrt{a_2 - \frac{i\mu}{2\nu}} \left[t_{12} - \frac{\nu b_2 - is}{2\nu a_2 - i\mu} \right] \right) \left. \right\}^* \quad (40)
\end{aligned}$$

The case $a_2 = 0$ corresponds to the combination of a finite time chirp and a finite time sinusoidal signal shown in one of the figures below.

(iv) *Graphical illustrations*

We have plotted $M(s, \mu, \nu)$ for some signals. In all cases we use μ and ν as in Eq.(5) with $T = 1$ and $\Omega = 10$. All signals are finite time signals and in each case we display a three-dimensional and a contour plot.

Figs 1a,b. The signal is

$$f(t) = \begin{cases} e^{-i20t} + e^{i10t} & t \in (0, 1) \\ 0 & t \notin (0, 1) \end{cases} \quad (41)$$

Although the number of periods, during which is signal is on, is relatively small, the two contributing frequencies are clearly seen in the separating ridges.

Figs 2a,b. The signal is

$$f(t) = \begin{cases} e^{-i20t} & t \in (0, \frac{1}{4}) \\ 0 & t \in (\frac{1}{4}, \frac{3}{4}) \\ e^{i10t} & t \in (\frac{3}{4}, 1) \end{cases} \quad (42)$$

Once again the contributions separate as θ grows, but notice the intermediate interference region which is a signature of the time-sequence of the frequencies occurrence and of their relative phase.

Figs 3a,b. The signal is

$$f(t) = \left\{ \begin{array}{ll} e^{-i(20t+10t^2)} + e^{i10t} & t \in (0, 1) \\ 0 & t \notin (0, 1) \end{array} \right\} \quad (43)$$

Contrasts the signature shapes of a chirp contribution and a regular sinusoidal pulse.

Notice that all $M(s, \theta)$ values have a probability interpretation. Therefore all peaks or oscillations have a direct physical meaning and, as opposed to the time-frequency quasidistributions, we need not worry about spurious effects. This is particularly important for the detection of signals in noise, as we will see in the next example.

(v) *Detection of noisy signals by NCT*

In Fig.4a and 4b we have plotted a time signal $f(t)$ and its spectral density $|f(\omega)|^2$. It is really very hard to decide, from these plots, where this signal might have originated from. Now we plot the NCT transform (Fig.4c) and its contour plot (Fig.4d) with the normalization $T = 1$ and $\Omega = 1000$. It still looks quite complex but, among all the peaks, one may clearly see a sequence of small peaks connecting a time around 0.5 to a frequency around 200.

In fact the signal was generated as a superposition of a normally distributed random amplitude and random phase noise with a sinusoidal signal of the same average amplitude but operating only during the time interval (0.45,0.55). This means that, during the observation time, the signal to noise power ratio is 1/10. The signature that the signal leaves on the NCT transform is a manifestation of the fact that, despite its low SNR, there is a number of particular directions in the (t, ω) plane along which detection happens to be more favorable. The reader may convince himself of the soundness of this interpretation by repeating the experiment with different noise samples and noticing that each time the coherent peaks appear at different locations, but the overall geometry of the ridge is the same.

Of course, to rely on a ridge of small peaks for detection purposes only makes sense because the rigorous probability interpretation of $M(s, \theta)$ renders the method immune to spurious effects.

4 NCT for other non-commuting pairs. The time-scale and frequency-scale cases

The method may also be applied to other pairs of non-commuting variables for which, as in the time-frequency case, there cannot be a joint probability density. Consider the pair time-scale, where scale is the operator

$$D = \frac{1}{2} (t\omega + \omega t) = \omega t + \frac{i}{2} \quad (44)$$

In the plane (t, D) we consider the linear combination

$$s_1 = \mu t + \nu D = \frac{\cos \theta}{T} t + \nu D \quad (45)$$

The relevant characteristic function is

$$\begin{aligned} C_{\mu\nu}^{(1)}(k) &= \langle e^{ik(\mu t + \nu D)} \rangle = \int f^*(t) e^{ik(\mu t + \nu D)} f(t) dt \\ &= \int f^*(e^{-\frac{k\nu}{2} t}) e^{i2\frac{\mu}{\nu} \sinh(\frac{k\nu}{2})} f(e^{\frac{k\nu}{2} t}) dt \end{aligned} \quad (46)$$

and the NCT transform is, as before, the Fourier transform of $C_{\mu\nu}^{(1)}(k)$

$$M^{(1)}(s_1, \mu, \nu) = \frac{1}{2\pi} \int C_{\mu\nu}^{(1)}(k) e^{-iks_1} dk$$

leading to

$$\begin{aligned} M^{(1)}(s_1, \mu, \nu) &= \frac{1}{2\pi|\nu|} \left| \int_{t>0} \frac{dt}{\sqrt{t}} f(t) e^{i\left(\frac{\mu}{\nu} t - \frac{s_1}{\nu} \log t\right)} \right|^2 + \\ &\quad \frac{1}{2\pi|\nu|} \left| \int_{t<0} \frac{dt}{\sqrt{|t|}} f(t) e^{i\left(\frac{\mu}{\nu} t - \frac{s_1}{\nu} \log|t|\right)} \right|^2 \end{aligned} \quad (47)$$

For the pair frequency-scale, (ω, D) , we obtain similarly

$$s_2 = \mu\omega + \nu D = \frac{\cos \theta}{\Omega} \omega + \nu D \quad (48)$$

$$\begin{aligned} M^{(2)}(s_2, \mu, \nu) &= \frac{1}{2\pi|\nu|} \left| \int_{\omega>0} \frac{d\omega}{\sqrt{\omega}} f(\omega) e^{-i\left(\frac{\mu}{\nu} \omega - \frac{s_2}{\nu} \log \omega\right)} \right|^2 + \\ &\quad \frac{1}{2\pi|\nu|} \left| \int_{\omega<0} \frac{d\omega}{\sqrt{|\omega|}} f(\omega) e^{-i\left(\frac{\mu}{\nu} \omega - \frac{s_2}{\nu} \log|\omega|\right)} \right|^2 \end{aligned} \quad (49)$$

$f(\omega)$ being the Fourier transform of the signal $f(t)$.

References

- [1] L. Cohen, " *Time-frequency distributions - A review*", Proc. IEEE, vol.77, pp. 941-981, 1989.
- [2] G. Faye Boudreaux-Bartels, " *Mixed time-frequency signal transformations*" in " *The transforms and applications handbook*", A. D. Poularikas (Ed.), pp. 887-962, CRC Press, Boca Raton 1996.
- [3] E. Wigner, " *On the quantum correction for thermodynamic equilibrium*", Phys. Rev. vol.40, pp. 749-759, 1932.
- [4] J. Ville, " *Théorie et applications de la notion de signal analytique*", Cables et Transmission, vol.2A, pp. 61-74, 1948.
- [5] L. Cohen and T. Posch, " *Positive time-frequency distribution functions*", IEEE Trans. Acoust., Speech, Signal Processing, vol. 33, pp. 31-38, 1985.
- [6] K. Vogel and H. Risken, " *Determination of quasiprobability distributions in terms of probability distributions for the rotated quadrature phase*", Phys. Rev. vol.A40, pp. 2847-2849, 1989.
- [7] S. Mancini, V. I. Man'ko, and P. Tombesi, " *Wigner function and probability distribution for shifted and squeezed quadratures*" Quantum Semi-class. Opt. vol.7, pp. 615-623, 1995.
- [8] S. Mancini, V.I. Man'ko, and P. Tombesi, " *Symplectic tomography as classical approach to quantum systems*", Phys. Lett. vol.A213, pp. 1-6, 1966.
- [9] S. Mancini, V.I. Man'ko, and P. Tombesi, " *Classical-like description of quantum dynamics by means of symplectic tomography*", Found. Phys. vol.27, pp.801-824, 1997.
- [10] V.V. Dodonov, E.V. Kurmyshev, and V.I. Man'ko, " *Generalized uncertainty relations and correlated coherent states*" Phys. Lett. vol.A79, pp. 150-152, 1980.
- [11] E.C.G. Sudarshan, Charles B. Chiu, and G. Bhamathi, " *Generalized uncertainty relations and characteristic invariants for the multimode states*" Phys. Rev. vol.A52, pp. 43-54, 1995.

- [12] H.P. Yuen, " *Two-photon coherent states of the radiation field*", Phys. Rev. vol.A13, pp. 2226-2243, 1976.
- [13] D.F. Walls, " *Evidence for the quantum nature of light*", Nature vol.280, pp. 451-454, 1979.

Fig.1A

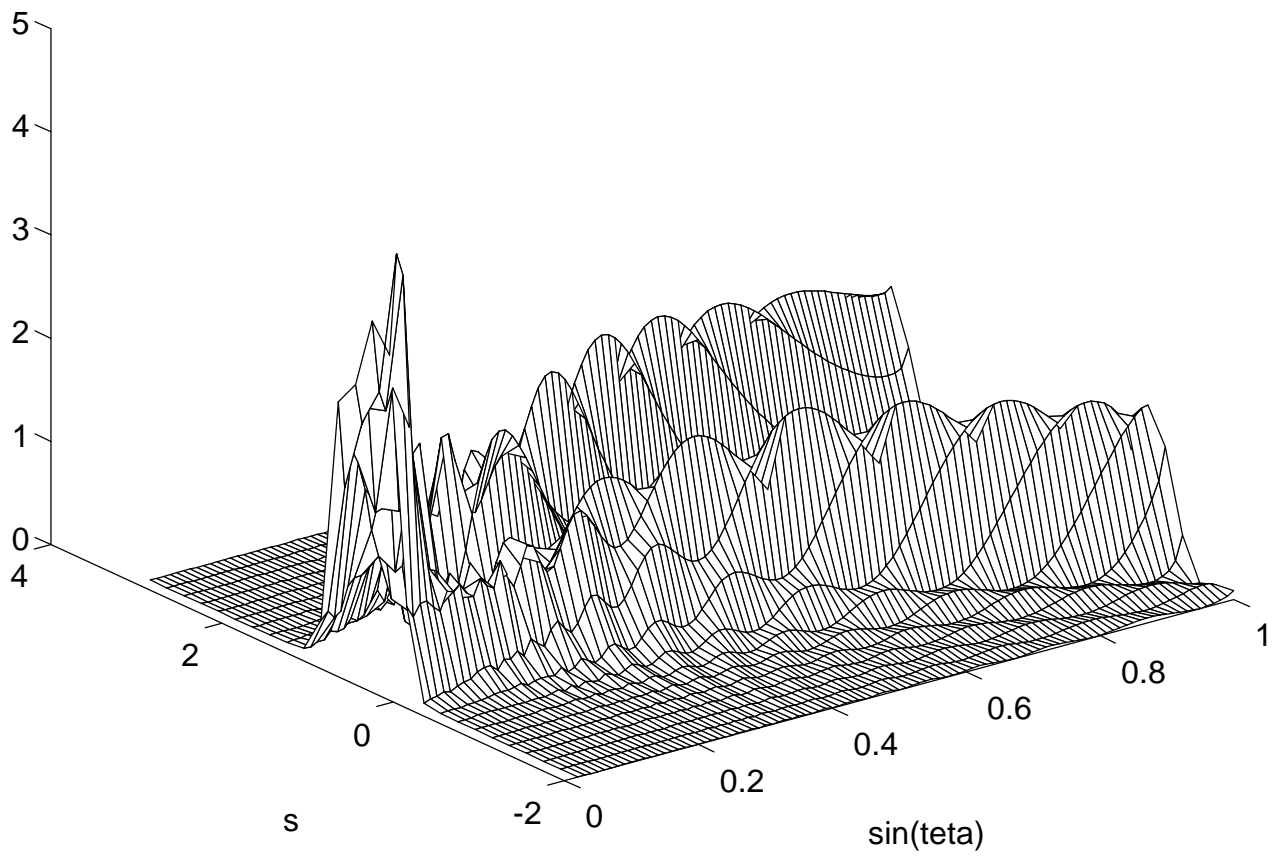


Fig.1B

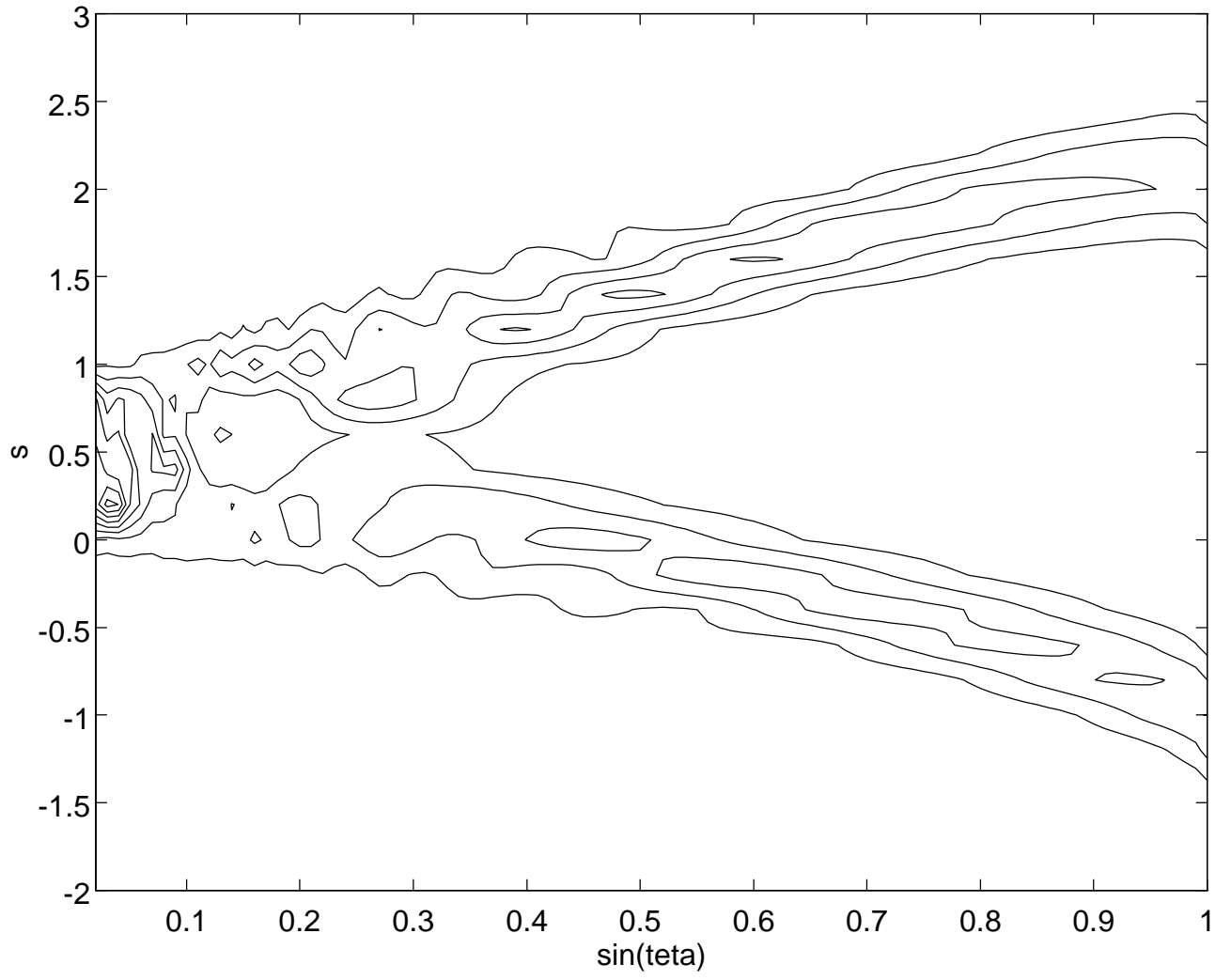


Fig.2A

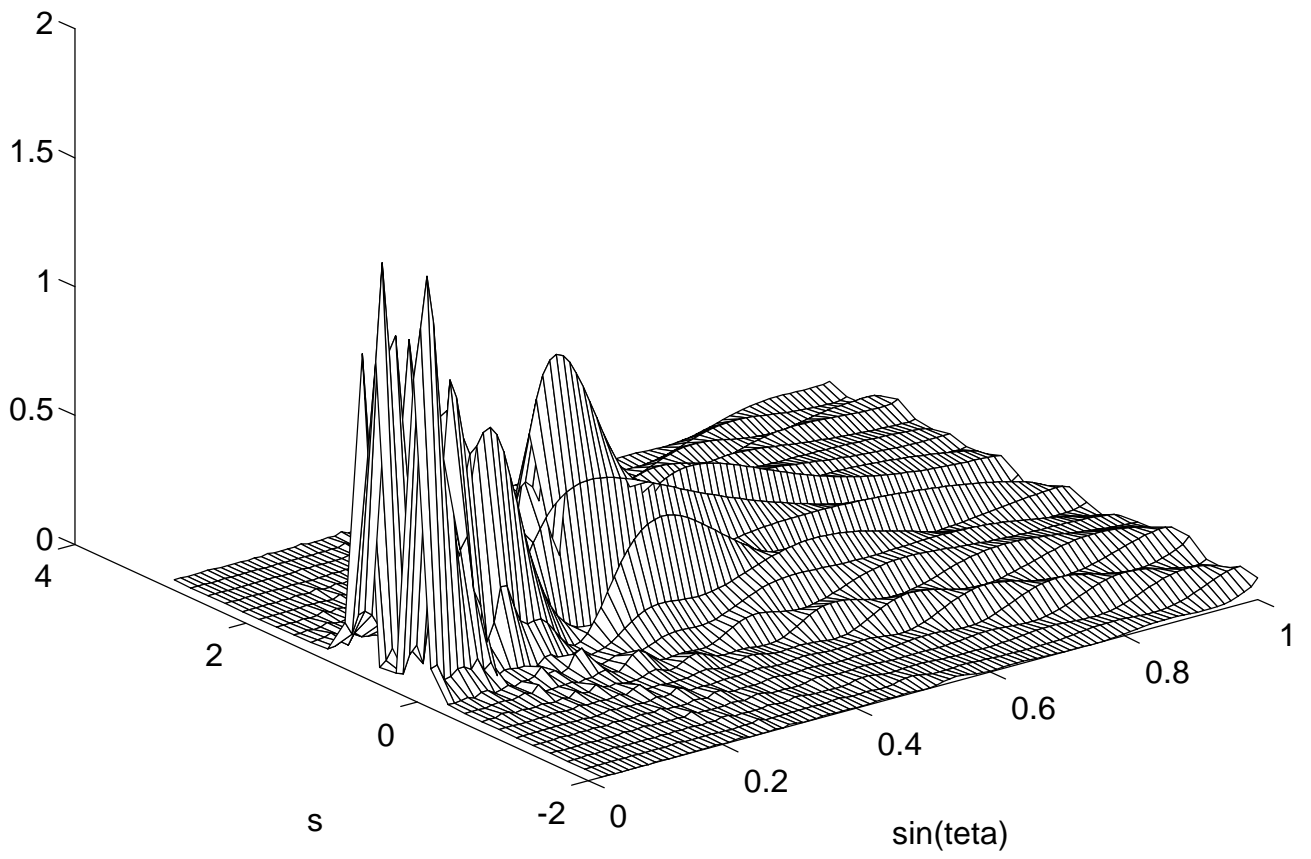


Fig.2B

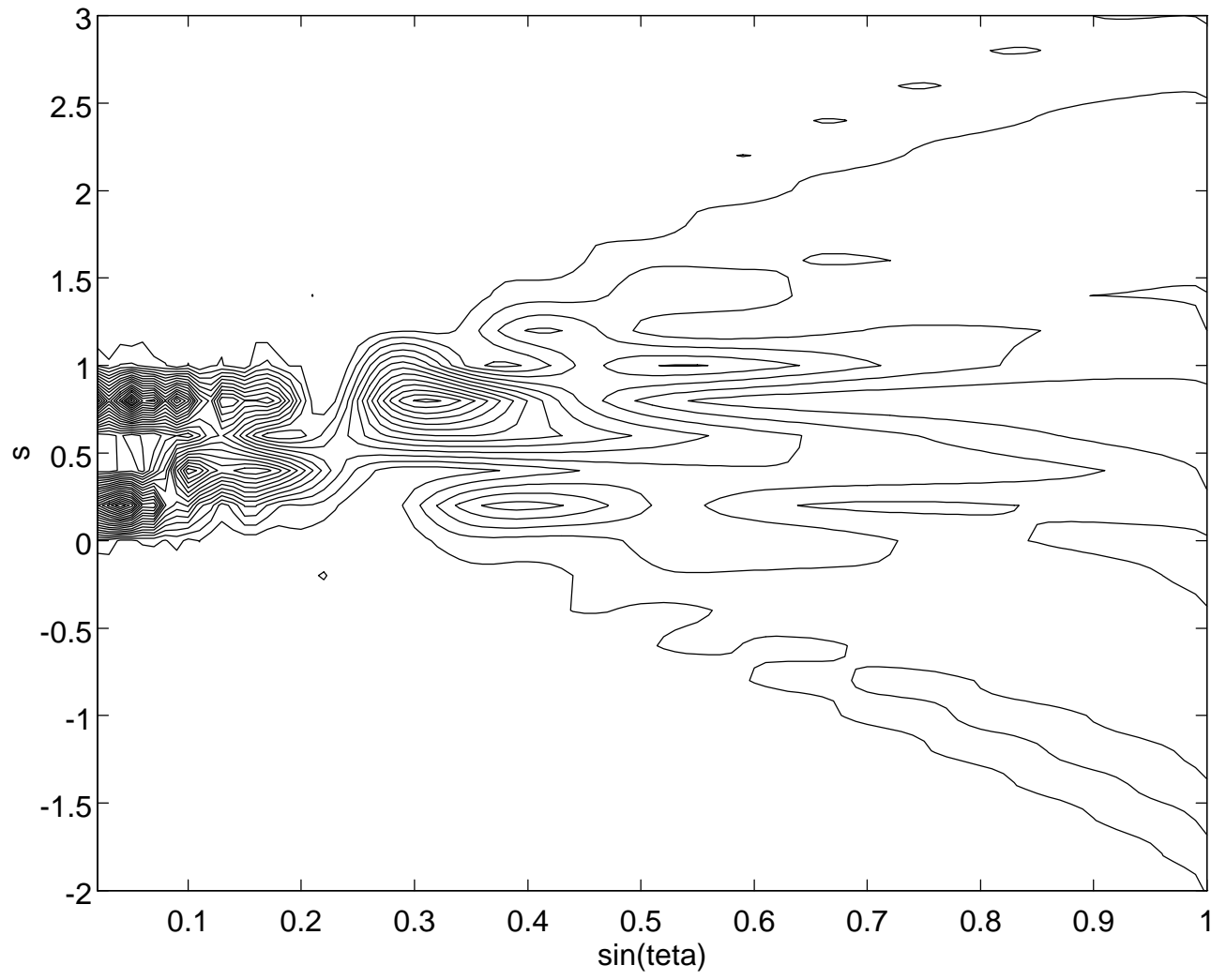


Fig.3A

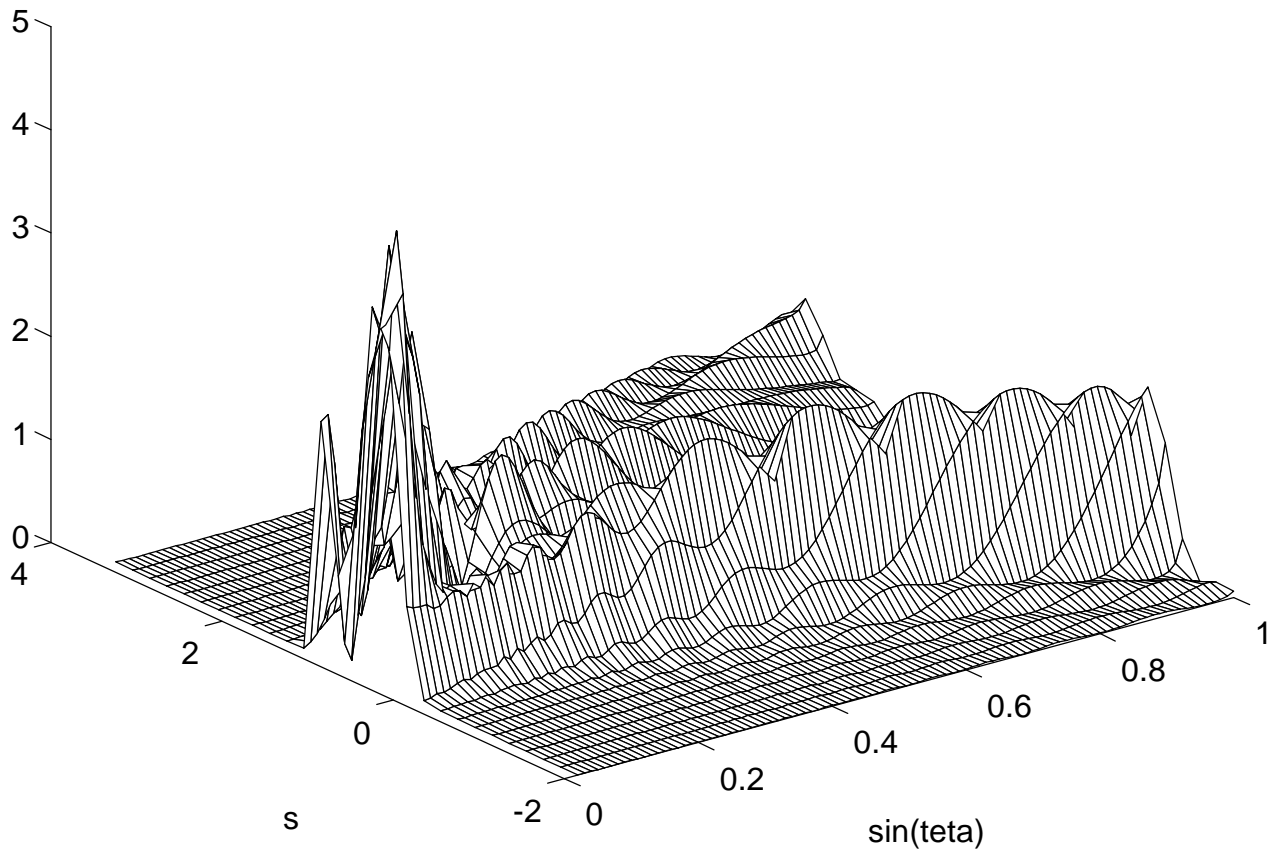


Fig.3B

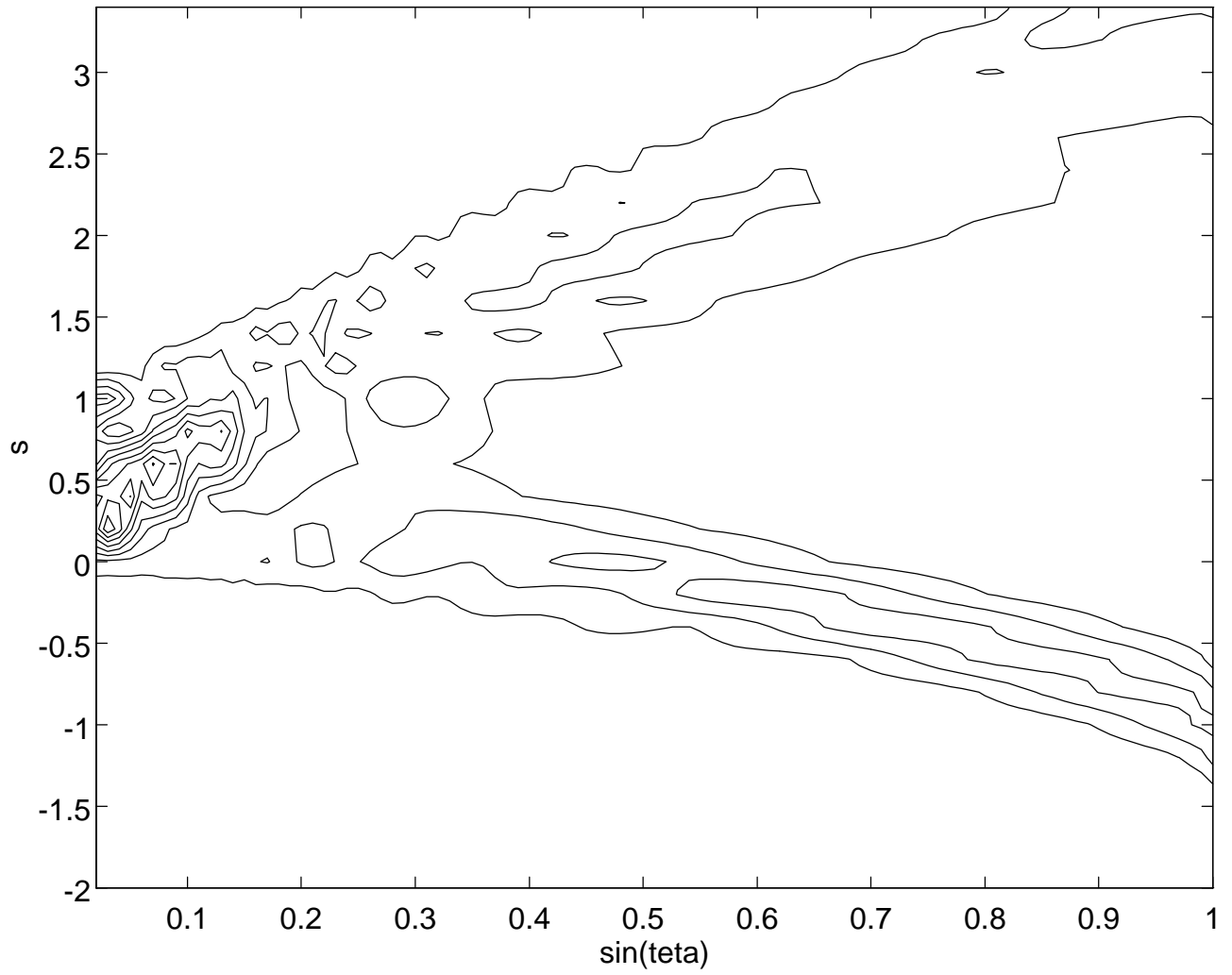


Fig.4A

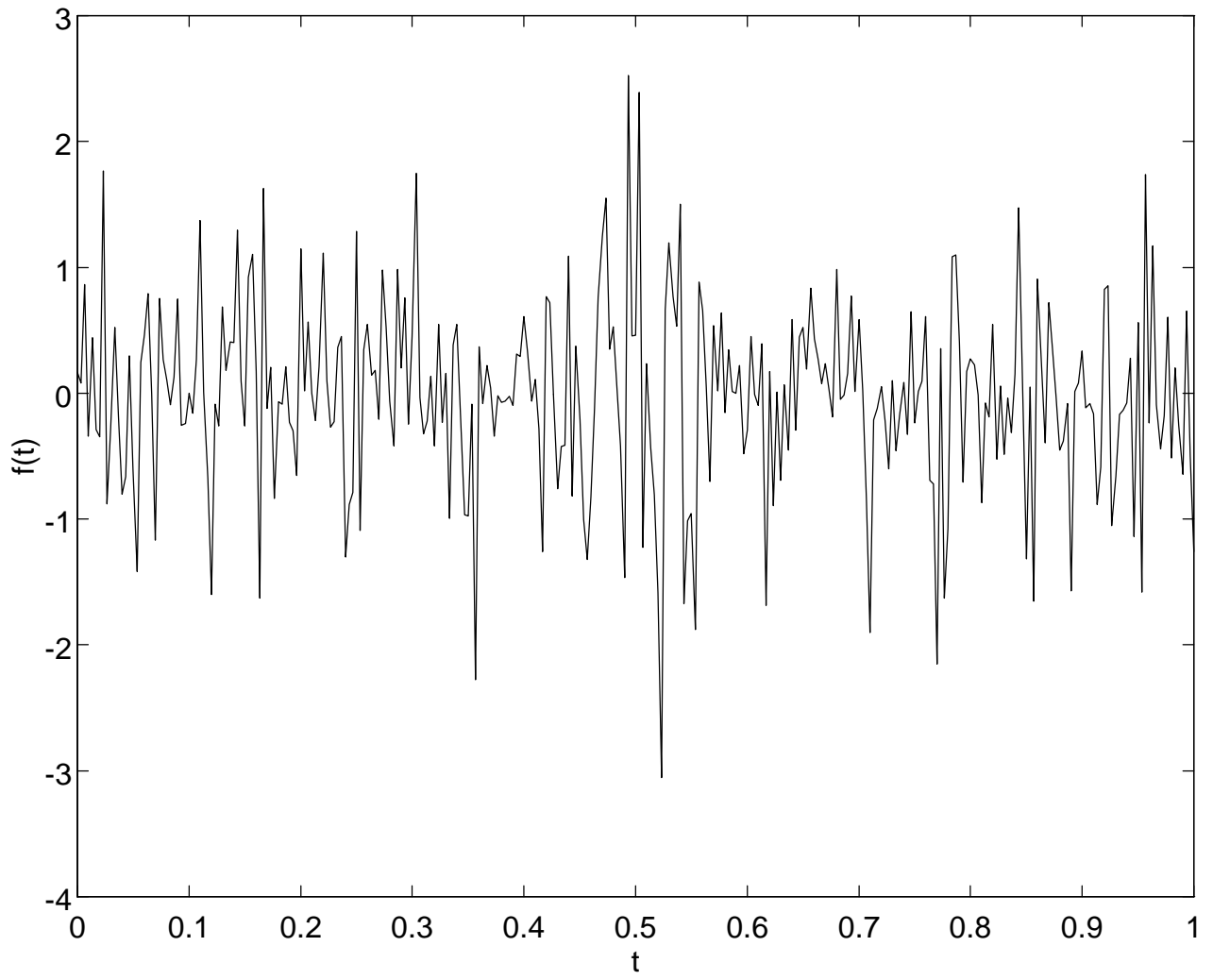


Fig.4B

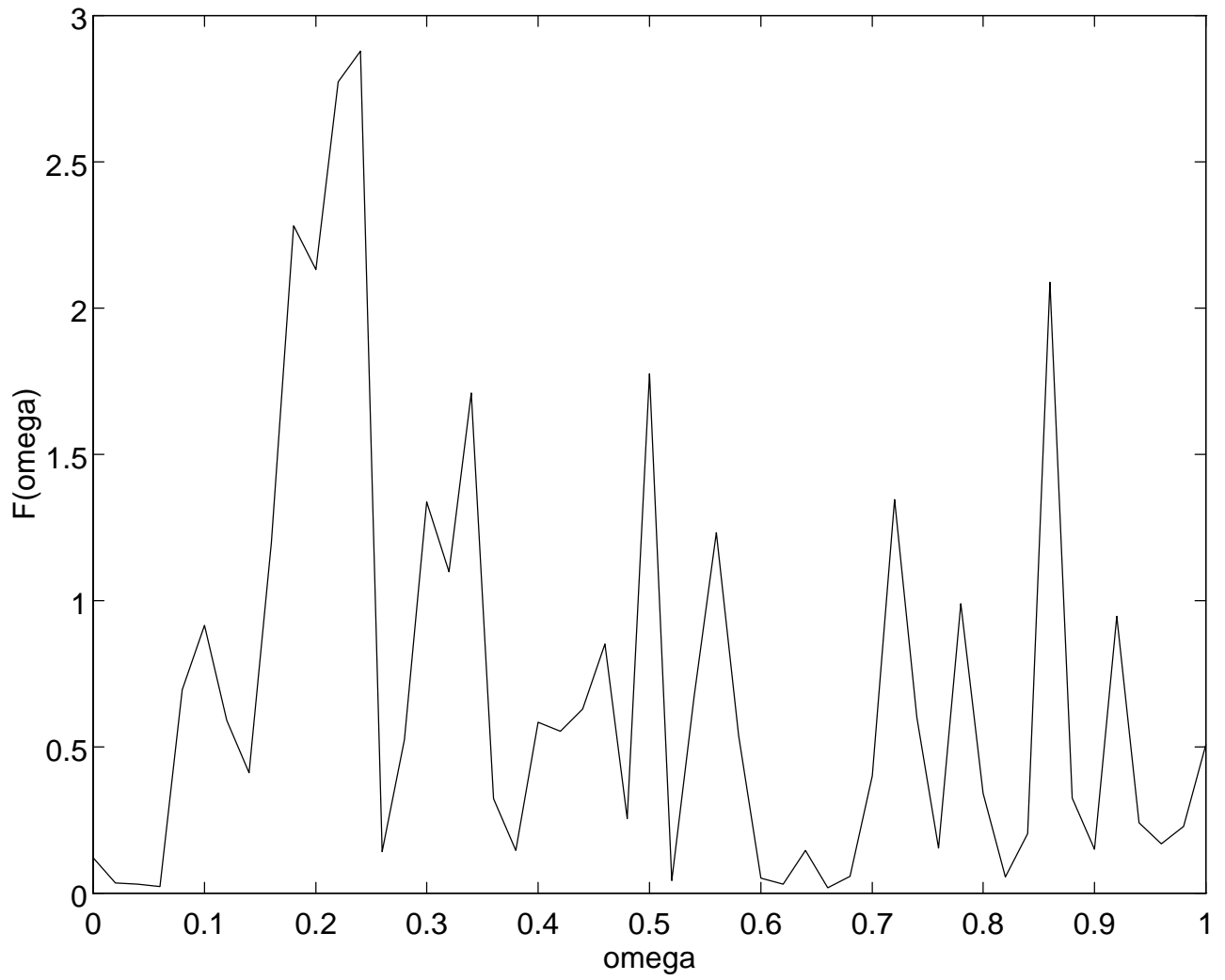


Fig.4C

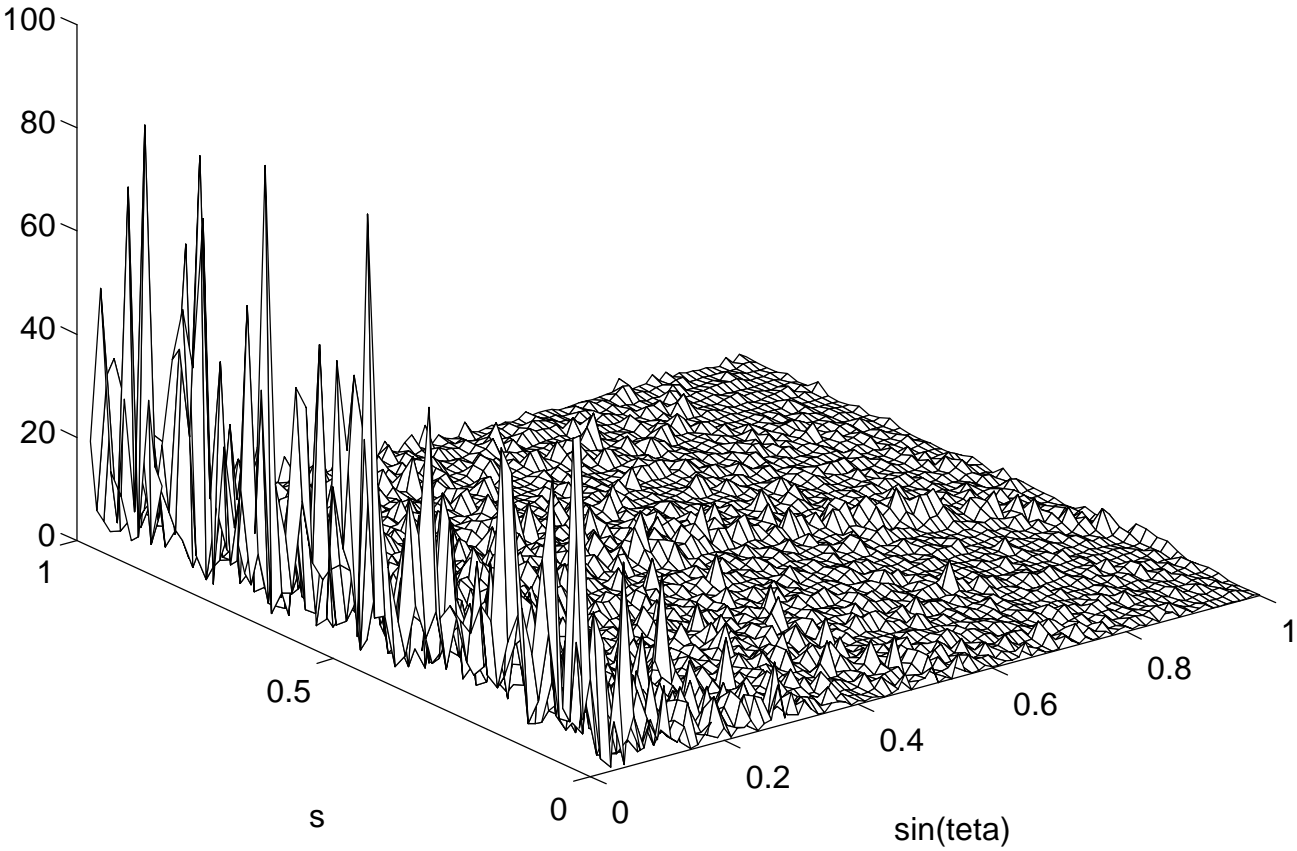


Fig.4D

